Magnetic Ordering of Magnetite Inclusions in Olivine at Mantle Depths in Subduction Zones

Marcello Campione,* Mara Murri, Valerio Cerantola, Dimitrios Bessas, Anja Rosenthal, Aleksandr Chumakov, Marco Scambelluri, and Nadia Malaspina*

Read Online

ACCESS | Metrics & More | Article Recommendations | Supporting Information

ABSTRACT: Magnetite microinclusions in metamorphic harzburgites, derived from the deserpentinization of the subducted hydrated oceanic lithospheric mantle, were examined by synchrotron Mössbauer spectroscopy to investigate the chemical and magnetic environments of the Fe nuclei. The data reveal a critical susceptibility of the octahedral sites of the cubic structure of magnetite to chemical variations, which, in turn, influences their magnetic properties in terms of hyperfine magnetic field intensity and direction. Micromagnetites display substantial remanent magnetization; however, the magnetic moment direction can be significantly different among inclusions, even for those in close spatial proximity. This evidence points to a kinetic control of the composition of microcavities at mantle depths, implying that the use of the remanent magnetic field of included magnetic phases to infer large-scale implications on the Earth's magnetic field requires the development of complex geochemical and geodynamical models.

KEYWORDS: synchrotron Mössbauer spectroscopy, serpentinization-induced magnetism, multiphase inclusions, geomagnetism, thermoremanent magnetization, chemical remanent magnetization, kinetically controlled process
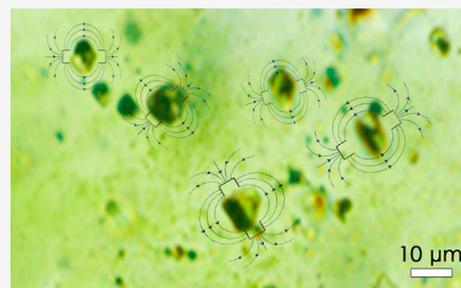
INTRODUCTION

The Earth's mantle has been traditionally considered "non-magnetic" because its thermal conditions usually exceed the Curie temperature of magnetite (580 °C, at ambient pressure). In the early 2000s, some studies demonstrated the occurrence of magnetic anomalies in the lithospheric mantle at those conditions where magnetite crystals can occur as needles inside olivine in xenolith samples from different geodynamic scenarios[1] and as crystals formed after the serpentinization of the so-called "cold nose" of the mantle wedge.[2] Also, the transition from magnetite to hematite along a (very) cold subduction zone may provide an additional source of magnetism to the mantle at depths of the transition zone.[3]

Magnetic iron oxides can exhibit remanent magnetization after cooling through their Curie temperature in the presence of the geomagnetic field and can preserve their magnetic state for billions of years, provided that the Curie temperature is not subsequently exceeded.[4,5] The increase of the Curie temperature of magnetite with pressure,[6,7] observed in laboratory experiments, bolstered the hypothesis that this mineral represents a primary source of upper mantle magnetization.[5] At mantle depths, magnetite can occur in multiphase solid inclusions crystallized from metamorphic fluids produced by the subduction zone dehydration of serpentinized mantle rocks. In this case, the breakdown reaction of antigorite at $p-T$ conditions of 1.5–2.2 GPa and 640–750 °C produces metamorphic olivine and orthopyroxene that trap the fluid

produced by dehydration.[8,9] Recent work[10] showed that magnetite inclusions in metamorphic olivine produced by this reaction are a unique case of commensurate epitaxial growth at mantle conditions: the magnetite–olivine interface displays parallelism between crystallographic planes $(111)_{Mag}$ and $(100)_{Ol}$ and between crystallographic directions $\langle 110 \rangle$ and $\langle 011 \rangle$, respectively (see the Petrographic Description and Figures S1 and S2 of the Supporting Information). As a result of these robust structural constraints, these samples are therefore ideal to study the relationship between the crystallographic ordering and the magnetic ordering of isolated single magnetite microcrystals formed along a subduction zone at upper mantle depths and temperatures exceeding those of the serpentinized cold mantle wedge.

Crystallographically oriented and magnetized magnetite inclusions are expected to strongly affect the features of nuclear resonance spectra, such as those collected with synchrotron Mössbauer spectroscopy (SMS), because of the intrinsic polarization of synchrotron radiation. The SMS spectrum at room temperature of magnetite consists of two

partially overlapped Zeeman split sextets. One sextet is assigned to tetrahedrally coordinated Fe^{3+} ("A" sites). The other sextet is assigned formally to $Fe^{2.5+}$ in an octahedral environment ("B" sites). Anisotropy of SMS spectra might be indicated by the dependence of spectral line intensity upon the relative orientation of the hyperfine field vector at the nucleus $\mathbf{H}_{hf}$ and the beam direction and polarization plane orientation (see the Experimental Methods of the Supporting Information).

Different hyperfine magnetic field directions in identically oriented crystals imply an extraordinary variation of the surrounding magnetic field during retrograde paths experienced by the rock (thermoremanent magnetization) and/or during crystal nucleation and growth (chemical remanent magnetization) and require a proper investigation, because the underlying causes might reflect the orientation of the geomagnetic field at mantle depths in specific time intervals during Earth's evolution.

The robust constraints on the orientation of magnetite microcrystals within a single olivine domain in our samples provide strong constraints on the possible texture effects[11] on SMS spectra. We extracted the hyperfine magnetic field strength and orientation distribution in naturally oriented single magnetite inclusions in olivine using SMS. Sets of inclusions in close spatial proximity were selected to ensure that they experienced the same $p-T$ path. Under these conditions, any variability is attributed to exogenous variations of the external magnetic field direction that occurred during the inclusion evolution.

■ SAMPLES AND METHODOLOGY

We studied of a total set of 22 micromagnetite (Mag) inclusions of size ranging from 2.5 to 5 μm distributed in two rock sections (14 in AL9564b1 and 8 in AL9564b2) of metamorphic harzburgites from the Almirez Complex.

We collected SMS spectra at ID18, the nuclear resonance beamline of the European Synchrotron Radiation Facility (ESRF). Acquisition of SMS data is described in detail in the Supporting Information.

■ RESULTS

Figure 1 shows a set of Mag inclusions in olivines measured by SMS. SMS spectra were collected by positioning the X-ray beam at places where optical images depict a black spot identifying the presence of a Mag inclusion. In these cases, the collected Mössbauer spectra show 12 absorption lines corresponding to the two sextets as a result of the A and B sites in a cubic magnetite crystal and, in addition, two intense absorption lines close to the abscissa origin as a result of the host olivine crystals.

A thorough fitting of a total set of Mag inclusions permitted us to evaluate isomer shift (IS) and hyperfine magnetic fields (H_{hf}) for both the A and B sites, as reported in Figure 2. Despite these parameters being consistent with those expected for magnetite single crystals ($IS_A = 0.27$ mm s^{-1}, $IS_B = 0.67$ mm s^{-1}, $H_{hf\,A} = 49$ T, and $H_{hf\,B} = 46$ T), a marked variability of the hyperfine magnetic field at octahedral sites ($H_{hf\,B}$) is observed (see also Table S1 of the Supporting Information).

In Mag, Fe(II)−Fe(III) pairs in octahedral sites (B) can oxidize to produce an Fe(III)−Fe(III) pair and a vacancy (V), so that the formula can be written as $(Fe^{3+})_A(Fe_{2(1-3x)}{}^{2.5+}Fe_{5x}{}^{3+}V_x)_BO_4$, where $0 < x < 0.33$, or
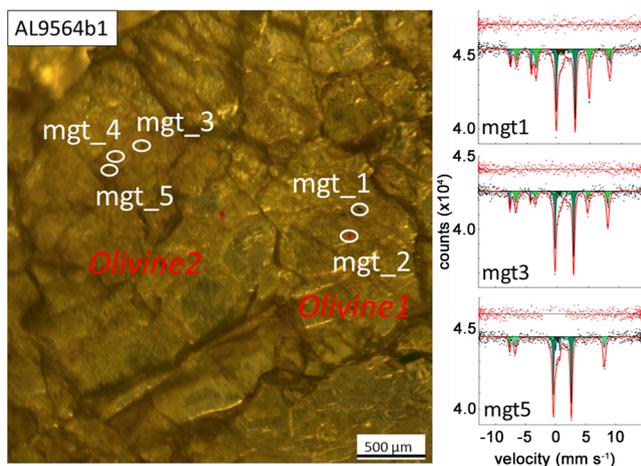

Figure 1. (Left) Optical micrograph showing a set of measured magnetite inclusions with indication of their IDs, olivine domain (red), and section name (top left). (Right) SMS spectra collected in transmission geometry through the olivine domains containing Mag 1, 3, and 5. Spectra are distinguished on the basis of the ratio among the relative areas of the six lines sextet 3:p:1:1:p:3, where $p \cong 4$ (Mag 1), $p \cong 2$ (Mag 3), and $p \cong 0$ (Mag 5).

simply $Fe_{3-x}O_4$. In this case, the signal of the B sextet decreases with oxidation, while the new Fe(III) signal cannot be distinguished from that of the tetrahedral site (A). Hence, the sextet area ratio ($S_B/S_A = R$) is indicative of the ratio $Fe^{2.5+}/Fe^{3+}$. As a result of the Mössbauer fraction of $Fe^{2.5+}$ on the B sites being somewhat lower than that of Fe^{3+} on the A sites,[12] the sextet area ratio of stoichiometric magnetite (R_0) at room temperature is not 2:1 but 1.8:1 and decreases with x in accordance with the following relation:

$$R = \frac{S_B}{S_A} = \frac{R_0(1 - 3x)}{1 + 5x} \qquad (1)$$

Values of $R > 1.8$ are attributed to the formation of the solid solution $Fe_{3-y}Ti_yO_4$ ($Fe_3O_4/Fe_2{}^{2+}TiO_4$), arising from an isomorphic substitution of Fe^{3+} by Ti^{4+}, bringing about a relative increase of Fe^{2+} to maintain charge balance. The oxidation of titanomagnetites, in turn, brings about the formation of titanomaghemite, $Fe_{(3-y)r}Ti_{yr}V_{3(1-r)}O_4$, with $r = 8/[8 + z(1 + y)]$, where z is the oxidation parameter, $0 < z < 1$,[13] yielding a decrease of the value of R. Hence, the same value of R can be attained in systems with substantial differences in terms of the content of Ti and excess oxygen.

Figure 3 reports the R values for the whole set of Mag inclusions measured in this study. As seen, some Mag inclusions show a variability mostly within the experimental uncertainties in their composition and oxidation state. This variability, similar to that observed for H_{hf} (Figure 2), is attributed to the characteristic susceptibility to chemical substitution on the B sites.

Once the intensity of the olivine matrix signal is taken into account, the relative areas of the six lines that form the sextet of Mag inclusions (Figure 1) are correlated to the Fe magnetic moment direction relative to the X-ray beam direction and polarization (Figure S4 of the Supporting Information; the Fe magnetic moment is antiparallel to the ^{57}Fe hyperfine magnetic field vector). In the case of a random distribution of the orientations of the Fe magnetic moments, one expects a relative ratio of the six lines of 3:p:1:1:p:3, with $p = 2$. For
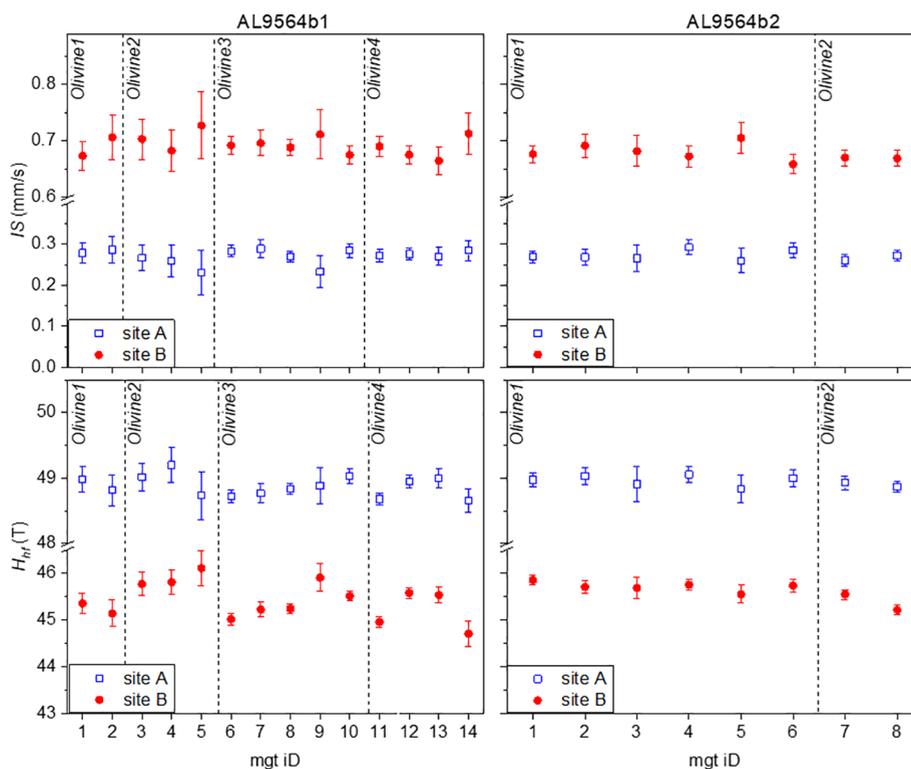
Figure 2. Isomer shift (IS) and hyperfine field (H_{hf}) of the A and B sites as deduced from fitting the SMS spectra of the magnetite inclusions.

magnetic moments homogeneously distributed within the plane perpendicular to the X-ray beam direction, a ratio approaching 3:4:1:1:4:3 (i.e., $p = 4$) is expected, while for a preferential alignment of the magnetic moment along a direction parallel to the X-ray beam direction, a ratio approaching 3:0:1:1:0:3 (i.e., $p = 0$) is expected. We emphasize that, as shown in Figure 1, the ensemble of Mag inclusions explored in this study, despite their spatial proximity, span all types of alignment. Figure 4 reports the distribution of p values ($p = 3/a_{12}$, where a_{12} is the ratio between the area of the first and second lines of the sextet; Figure S5 of the Supporting Information). Most experimental data are close to $p = 2$, corresponding to a random distribution of magnetic moments; however, substantial deviations are observed, both below and beyond $p = 2$, with a slight preference for $p < 2$, for both A and B sites.

DISCUSSION

The studied Mag inclusions, despite the homogeneity of the olivine matrix and their spatial proximity, span a wide range of compositions as a result of the variability of their Ti contents (Figure S6 of the Supporting Information), oxidation state, and vacancy concentration (Figure 3), with all these factors affecting the octahedral sites (B) of the microcrystals. This chemical variability impacts the nuclear magnetic state of ^{57}Fe atoms at B sites, which, in fact, display a remarkable variability of H_{hf} (Figure 2). These observations show that the evolution of the inclusion system is kinetically controlled: dissolution, oxidation, and reprecipitation processes are triggered by the contact with a fluid that is locally non-equilibrated and reactive with the associated solid phases.[10,14] The final local conditions between olivine, magnetite, and the fluid are dramatically dependent upon contingent factors, which vary from inclusion to inclusion: cavity shape and volume, presence of fractures,

permeability, proximity to exsolved phases, etc. We experimentally verified that some Mag inclusions display quite variable remanent magnetization directions. An interesting aspect is that different Mag inclusions in close spatial proximity sometimes exhibit substantial differences in their magnetization state (Figure 1). This means that, despite these inclusions experiencing the same prograde and retrograde $p-T$ path, they recorded a different magnetization. Because Mag forms at temperatures higher than the antigorite breakdown temperature (650 °C) and, therefore, also higher than the Curie temperature (600 °C for pure magnetite at 2 GPa),[6] the variability of their magnetization state is attributed to variations of their blocking temperature, which, in turn, depends upon both the size and shape of the microcrystals and the composition of magnetite in solid solution with ulvospinel. This implies that each Mag inclusion might have crossed the blocking temperature at different stages of the rock retrograde path or that the various Mag nucleated under different fluid/olivine interaction conditions and, thereby, acquired variable Ti contents.[15−17] The analyses performed by SMS allow us to attribute the possible difference of the blocking temperatures of Mag inclusions to their different compositions and stoichiometries.

Variations in the orientation of the local magnetic fields (Figure 4) can be the result of the (i) rototranslation of the rock during its pathway along the temperature gradient until it cools through the Curie point or (ii) inversion of the Earth's geomagnetic poles during motion of the rock. We finally consider as a possible though minor source of magnetic disorder, the chemical remanent magnetization recorded in Mag formed during retrograde serpentinization. However, this Mag is expected to be a very minor fraction of the total, as demonstrated in recent serpentinization experiments carried out in olivine cavities.[18]
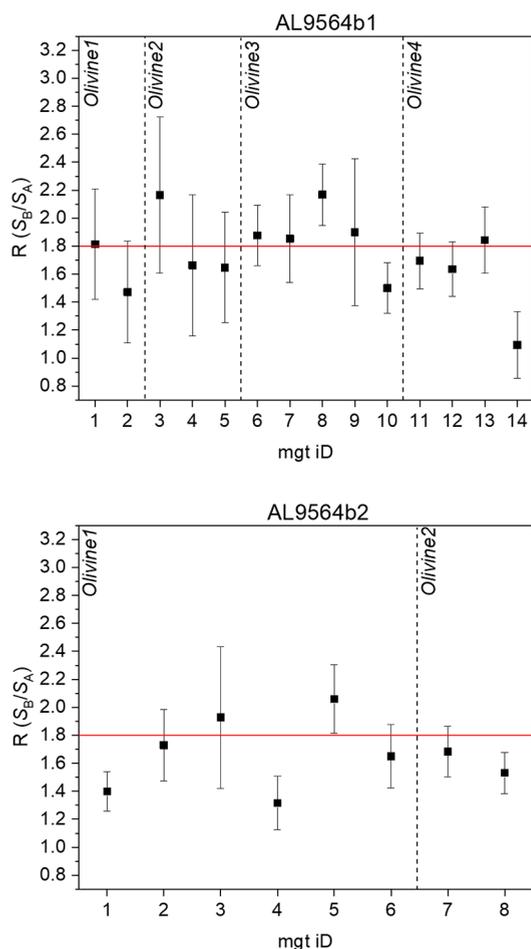
Figure 3. Ratio R of the areas of sextet B to sextet A areas obtained from SMS spectral fitting of the ensemble of Mag inclusions in sections AL9564b1 and AL9564b2. The horizontal line indicates the area ratio for stoichiometric magnetite at room temperature (1.8:1). Ratios higher than 1.8 are attributed to the isomorphic substitution of Fe^{3+} with Ti^{4+}, whereas oxidation leads to a reduction of R.

Figure 4. p values of the ensemble of the Mag belonging to the same section. The horizontal line is at $p = 2$, corresponding to magnetic disorder.

CONCLUSION

The occurrence of iron oxides in the mantle, used to identify possible magnetic anomaly sources, may derive from the oxidation of olivine, the serpentinization of the supra-subduction mantle wedge at forearc depth, and as the product of the fluid/olivine interaction during the subduction of a serpentinite at subarc depths, as in the studied samples. The in-depth SMS analysis of our Mag inclusions allowed us to conclude that these microinclusions of magnetite in minerals are the result of a kinetically controlled process. This is indicated by the variability of their composition and defect concentration together with their magnetic properties, especially with respect to the octahedral sites. This variability is responsible for a distribution of blocking temperatures: different Mag inclusions, even though at nearby positions, experience magnetization as a result of the geomagnetic field at different stages of the retrograde path. Hence, different Mag inclusions generally record a different orientation of the magnetization.

The non-equilibrium nature of the processes leading to the formation of magnetic mineral inclusions at mantle depths implies that a number of chemical kinetic features can play local control o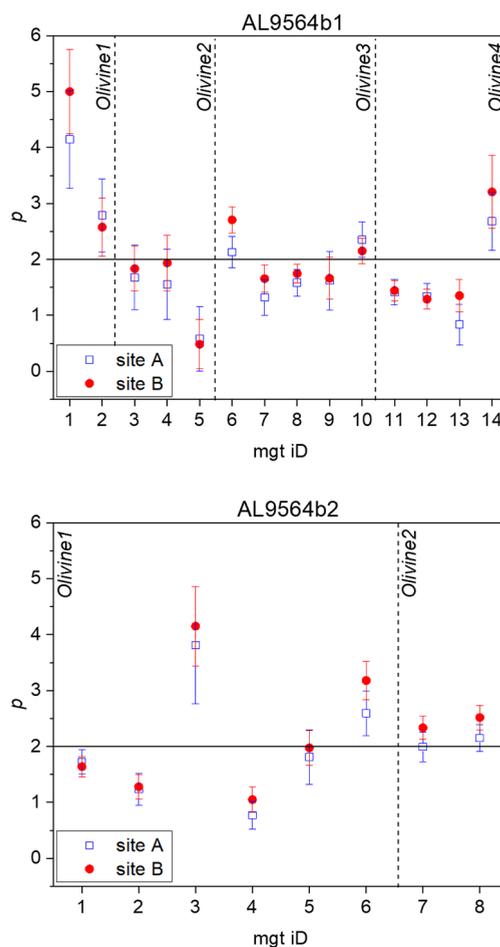n the remanent magnetic field recorded by this dehydration-controlled magnetite. Considering that this could be a diffuse process affecting the serpentinized mantle of subducting slabs and associated forearc mantle, caution must be used when utilizing the residual magnetic field to infer large-scale implications for the Earth's magnetic field.

ASSOCIATED CONTENT

ⓢ Supporting Information

The Supporting Information is available free of charge at https://pubs.acs.org/doi/10.1021/acsearthspace-chem.2c00190.

> Petrographic descriptions, experimental methods, chemical physical parameters of Mag inclusions (Table S1), optical micrographs of inclusions (Figure S1), crystallographic orientation of micromagnetite inclusions in olivine (Figure S2), optical micrographs of the two investigated sections (Figure S3), variation of the SMS spectrum with sample azimuthal rotation (Figure S4), area ratio of SMS line 1 over line 2 of the ensemble of investigated Mag (Figure S5), analysis of Mg, Fe, and Ti contents in Mag (Figure S6), and references (PDF)

AUTHOR INFORMATION

Corresponding Authors

Marcello Campione − *Department of Earth and Environmental Sciences, University of Milano-Bicocca, 20126*

Milano, Italy; ● orcid.org/0000-0001-5627-6186;
Email: marcello.campione@unimib.it

Nadia Malaspina − *Department of Earth and Environmental Sciences, University of Milano-Bicocca, 20126 Milano, Italy;*
● orcid.org/0000-0002-7089-1035;
Email: nadia.malaspina@unimib.it

Authors

Mara Murri − *Department of Earth and Environmental Sciences, University of Milano-Bicocca, 20126 Milano, Italy;*
● orcid.org/0000-0002-7149-9940

Valerio Cerantola − *Department of Earth and Environmental Sciences, University of Milano-Bicocca, 20126 Milano, Italy; European X-ray Free-Electron Laser, 22869 Schenefeld, Germany*

Dimitrios Bessas − *ESRF−The European Synchrotron, Grenoble 38000, France*

Anja Rosenthal − *ESRF−The European Synchrotron, Grenoble 38000, France; Research School of Earth Sciences, The Australian National University, Canberra, Australian Capital Territory 2601, Australia;* ● orcid.org/0000-0003-3912-4046

Aleksandr Chumakov − *ESRF−The European Synchrotron, Grenoble 38000, France;* ● orcid.org/0000-0002-0755-0422

Marco Scambelluri − *Department of Earth, Environment and Life Sciences, University of Genova, 16132 Genova, Italy*

Complete contact information is available at:
https://pubs.acs.org/10.1021/acsearthspacechem.2c00190

Notes

The authors declare no competing financial interest.

■ REFERENCES

(1) Ferré, E. C.; Friedman, S. A.; Martín-Hernández, F.; Feinberg, J. M.; Conder, J. A.; Ionov, D. A. The Magnetism of Mantle Xenoliths and Potential Implications for Sub-Moho Magnetic Sources. *Geophys. Res. Lett.* **2013**, *40* (1), 105−110.

(2) Blakely, R. J.; Brocher, T. M.; Wells, R. E. Subduction-Zone Magnetic Anomalies and Implications for Hydrated Forearc Mantle. *Geology* **2005**, *33* (6), 445−448.

(3) Kupenko, I.; Aprilis, G.; Vasiukov, D. M.; McCammon, C.; Chariton, S.; Cerantola, V.; Kantor, I.; Chumakov, A. I.; Rüffer, R.; Dubrovinsky, L.; Sanchez-Valle, C. Magnetism in Cold Subducting Slabs at Mantle Transition Zone Depths. *Nature* **2019**, *570* (7759), 102−106.

(4) Piazzi, M.; Morana, M.; Coïsson, M.; Marone, F.; Campione, M.; Bindi, L.; Jones, A. P.; Ferrara, E.; Alvaro, M. Multi-Analytical Characterization of Fe-Rich Magnetic Inclusions in Diamonds. *Diam. Relat. Mater.* **2019**, *98*, 107489.

(5) Ferré, E. C.; Kupenko, I.; Martín-Hernández, F.; Ravat, D.; Sanchez-Valle, C. Magnetic Sources in the Earth's Mantle. *Nat. Rev. Earth Environ.* **2021**, *2* (1), 59−69.

(6) Schult, A. Effect of Pressure on the Curie Temperature of Titanomagnetites [(1 − x) · Fe₃O₄ − x · TiFe₂O₄]. *Earth Planet. Sci. Lett.* **1970**, *10* (1), 81−86.

(7) Samara, G. A.; Giardini, A. A. Effect of Pressure on the Néel Temperature of Magnetite. *Phys. Rev.* **1969**, *186* (2), 577−580.

(8) Trommsdorff, V.; López Sánchez-Vizcaíno, V.; Gómez-Pugnaire, M. T.; Müntener, O. High Pressure Breakdown of Antigorite to Spinifex-Textured Olivine and Orthopyroxene, SE Spain. *Contrib. Mineral. Petrol.* **1998**, *132* (2), 139−148.

(9) Scambelluri, M.; Bottazzi, P.; Trommsdorff, V.; Vannucci, R.; Hermann, J.; Gòmez-Pugnaire, M. T.; Lòpez-Sànchez Vizcaìno, V. Incompatible Element-Rich Fluids Released by Antigorite Breakdown in Deeply Subducted Mantle. *Earth Planet. Sci. Lett.* **2001**, *192* (3), 457−470.

(10) Campione, M.; La Fortezza, M.; Alvaro, M.; Scambelluri, M.; Malaspina, N. Commensurate Growth of Magnetite Microinclusions in Olivine under Mantle Conditions. *ACS Earth Space Chem.* **2020**, *4* (6), 825−830.

(11) Ericsson, T.; Wappling, R. Texture Effects In 3/2−1/2 Mössbauer Spectra. *J. Phys. Colloq.* **1976**, *37* (C6), C6-719−C6-723.

(12) *Mössbauer Spectroscopy*; Yoshida, Y., Langouche, G., Eds.; Springer: Berlin, Germany, 2013; DOI: 10.1007/978-3-642-32220-4.

(13) O'Reilly, W. The Identification of Titanomaghemites: Model Mechanisms for the Maghemitization and Inversion Processes and Their Magnetic Consequences. *Phys. Earth Planet. Inter.* **1983**, *31* (1), 65−76.

(14) Campione, M.; Tumiati, S.; Malaspina, N. Primary Spinel + Chlorite Inclusions in Mantle Garnet Formed at Ultrahigh-Pressure. *Geochem. Perspect. Lett.* **2017**, *4*, 19−23.

(15) Lattard, D.; Engelmann, R.; Kontny, A.; Sauerzapf, U. Curie Temperatures of Synthetic Titanomagnetites in the Fe-Ti-O System: Effects of Composition, Crystal Chemistry, and Thermomagnetic Methods. *J. Geophys. Res. Solid Earth* **2006**, *111* (12), B12S28.

(16) Mazo-Zuluaga, J.; Restrepo, J.; Mejía-López, J. Influence of Non-Stoichiometry on the Magnetic Properties of Magnetite Nanoparticles. *J. Phys.: Condens. Matter* **2008**, *20* (19), 195213.

(17) Smykatz-Kloss, W.Influence of the Chemical Composition on the Curie-Temperatures of Magnetites. In *Differential Thermal Analysis*; Wyllie, P. J., von Engelhardt, W., Hahn, T., Eds.; Springer: Berlin, Germany, 1974; Vol. *11*: Minerals and Rocks, pp 118−122, DOI: 10.1007/978-3-642-65951-5_18.

(18) Lamadrid, H. M.; Rimstidt, J. D.; Schwarzenbach, E. M.; Klein, F.; Ulrich, S.; Dolocan, A.; Bodnar, R. J. Effect of Water Activity on Rates of Serpentinization of Olivine. *Nat. Commun.* **2017**, *8* (1), 1−9.